Received: 9 May 2022 | Revised: 14 October 2022 | Accepted: 23 January 2023

DOI: 10.1002/poc.4494

RESEARCH ARTICLE

Journal of Physical Organic Chemistry WILEY

The adhesive energies between Poly(3-hexylthiophene) and Polyvinylpyrrolidone for organic electronic devices: Hybrid-exchange density-functional-theory studies

Xiaoyu Du | **Wei Wu** | **Kwang-Leong Choy**

UCL Institute for Materials Discovery, University College London, London, UK

Correspondence
Wei Wu and Kwang-Leong Choy, UCL Institute for Materials Discovery, University College London, Malet Place, WC1E 7JE London, UK.
Email: wei.wu@ucl.ac.uk and k.choy@ucl.ac.uk

Funding information
the EU Horizon 2020 Project Marketplace, Grant/Award Number: 760173

Abstract

Studying the building blocks for organic electronics—molecules—is important for achieving a great performance for organic electronic devices. Poly(3-hexylthiophene) (P3HT) and povidone (PVP) are common molecules chosen for the semiconducting and dielectric layers of organic electronic devices, respectively. Here, we have applied the hybrid-exchange density-functional theory, taking into account empirical dispersion forces and basis set superposition errors, to study the adhesive energies and optimal geometries when integrating the two types of molecules. To ease the analysis of the molecular structures, we have simplified the polymer chain structure to the monomer, dimer and trimer for the P3HT and PVP. By using B3LYP and BLYP functionals in combination with dispersion forces, we have found that the optimal inter-molecular vertical distances between P3HT and PVP are approximately 3.6, 6 and 5 Å for monomer, dimer and trimer, respectively, with the lowest adsorption energy of ∼−0.35, −0.15 and −0.45 eV. However, the sliding effect for the molecular combination is relatively small. These computational results can be potentially compared with the relevant experiments on the molecular crystal structure. The molecular orbitals of the P3HT and PVP molecules show that the charge density is mainly on the five-member rings rather than the polymer chains, which further supports our finite-chain approximation. Our calculations, especially the potential curves, could be useful for the optimal design of molecular structures for organic electronic devices.

KEYWORDS
density functional theory, hybrid exchange, organic electronics, P3HT, PVP

1 | INTRODUCTION

As a typical component for organic electronics, organic thin film transistors (OTFTs) are important for many emerging organic electronic devices. The high-end applications include light-emitting diodes,[1] radio frequency identification tags,[2] static random-access memory,[3] and e-paper.[4] The main elements in the OTFT include a source, a drain, an organic (active) layer (the main semiconductor part), a dielectric layer (also

called insulator), a gate and a substrate. Recently, wearable technologies, mostly taking advantage from organic electronics, have developed in an unprecedentedly rapid pace.[5] For most types of wearable devices, the electronic sensing components play an important role.[6] Sensing components can collect and transfer the environmental data such as temperature, pressure, smell and vibrations as electrical signals, which can then be received and processed by the other parts of the device.[7] Such typical organic sensor is normally composed of OTFT.[8,9] In the last few decades, carbon-based materials have been widely explored for semiconducting devices.[10] Comparing with the traditional silicon-based materials, they can be mechanically more flexible and stretchable, which can provide more functionalities in the real-world application of wearable devices.[11] For instance, nowadays, people are not satisfied with wearables in a rigid shape, which instead could be replaced by the smart clothes that can monitor the body temperature and movement. However, to fabricate such type of devices, we need to first identify the good candidate for the basic component, ideally mechanically flexible sensors, for which organic materials have great advantages owing to the material texture.[12]

Owing to the layered structure, the OTFT in the wearables can easily encounter problems at the interface, such as the scattering of the charge carriers.[13] One of the most common failures in such organic devices is the adhesive wear, which is defined as the material transfer between two layers locally at the interface.[14] Therefore, the distance between layers is a vital factor for the performance of OTFT. Poly(3-hexylthiophene) (P3HT, Figure 1A) and povidone (PVP, Figure 1B)[17] are the typical molecules currently used for the semiconductor and dielectric layers, respectively, in OTFT. Moreover, in addition to wearable technologies and sensors, OTFTs have a wide range of applications that need large area, flexible structures and low cost, such as active-matrix flat-panel displays, although they are not suitable for applications with fast switching speed.[18]

The research for the P3HT molecule has been very actively recently. Kuo et al.[19] have combined inorganic material zinc oxide with organic P3HT, which provided the boost of the mobility in the semiconductor (to as high as 24.7 $cm^2/V{\cdot}s$) and offered high sensitivity to gas, suggesting the potential of P3HT for sensors. It was then demonstrated that P3HT can be easily blended with another organic material, poly methyl methacrylate (PMMA), which was used as the dielectric layer.[20] In this research, the sensitivity of the OTFT to the nitrogen dioxide was much better than other traditional sensors, pointing to another branch of the OTFT applications. The team led by Aïssa[21] tested the performance of P3HT combined with single-walled carbon nanotubes (SWCNTs). Their experiments showed that the merits of these two materials can prompt with each other. Zhang et al.[22] used P3HT in the semiconductor layer of the OTFTs for the gas absorption. Apart from the mobility, P3HT was also proved to have good threshold voltage, which is another vital feature for the OTFT. In addition, in combination with metal−organic framework (MOF) materials, P3HT was also explored for absorbing air pollutants,[23] which is great for environment sustainability. P3HT was used for the active layer because its mobility is relatively high among the popular polymer semiconductor materials. It can vary from 0.0022 to 1.1 $cm^2/V{\cdot}s$ under different conditions.[24–29] Besides, P3HT also possesses good solubility[30] for the manufacture. As shown in Figure 1A, the backbone of P3HT will extend alongside the ring structure, with the extended alkane chain structure, which will help the polymer to form the lamellar structure. With this feature, when combined with another substrate, the orientation of P3HT will affect the performance of the active layer. However, with either the face-on or the edge-on orientation between the active layer and the substrate layer, the mobility can reach high values for P3HT, so this structure is favoured for the fabrication of semiconducting material.

For the PVPs, most of the recent studies have used them in a single layer, without combining with the other materials. Boukhili et al.[31] made a comparison among different dielectric materials, including PVP, divinyl tetramethyl disiloxane-bis (benzocyclobutene) (BCB) and poly (vinyl alcohol) (PVA), to evaluate different OTFT electrical properties. Koutsiaki et al.[32] studied the electrical performance on OTFTs with different thickness of dielectric layers, which showed that the mobility of the transistor would decrease when the dielectric layer became thicker; at the same time, the current leakage could be reduced to a small value. The stability of a sensor is essential because it may have an influence on the device lifespan. Hence, to study the variation of the

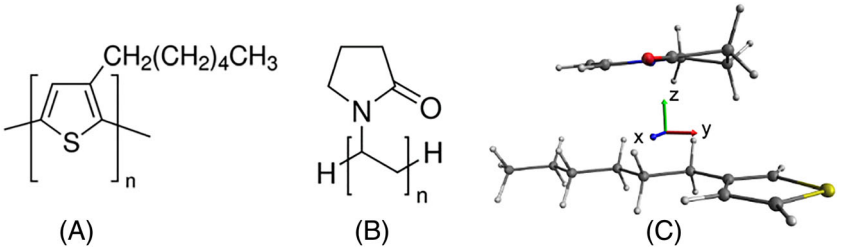

FIGURE 1 The molecule structures for P3HT[15] (A) and PVP[16] (B). (C) is an example of the combined molecular structure; the upper one is PVP monomer and the lower one is P3HT monomer.

performance under the exposure of air, Xie et al.[33] have performed the experimental work to compare dielectric layers with different thickness. The semiconductor layer was 2,7-dioctyl[1] benzothieno [3,2-b][1]benzothiophene (C8-BTBT), whereas the dielectric layer was PVP-hexafluoroisopropylidene diphthalic anhydride(HDA). The experimental results showed that with the moderate thickness (275 nm), the mobility and the threshold voltage can increase, whereas the on/off ratio can remain constant. This is a valuable study because it provided the reference thickness for future similar research, which can also be suitable for the flexible OTFT, with the normal condition that can be easily encountered in real life.

However, the research on the OTFT with P3HT as the semiconductor layer and PVP as the dielectric layer at the same time was rare. Hence, the study of this combination might be valuable for the future research and device design. Although there are not many organic materials that can be used as substrate layer, PVP stood out for its suitable characteristics as dielectric layers.[34] The most important feature is high dielectric constant as mentioned above, which can reach ~4.[32] PVP can also be fabricated along with a wide range of substrates and semiconducting materials, including glass, polymer and inorganic components.[35] Similar to P3HT, PVP has a good solubility,[36] which implies that it is chemically friendly to the organic solution procedures. Our research will therefore focus on the interaction between the P3HT in the semiconducting and the PVP molecules in the dielectric layers. The objective is to study the influence of inter-molecular distance on the interactions at the interface and try to find out the optimistic inter-molecular distance. Such calculations and the related analysis can be useful for the design of the OTFT based on the P3HT and PVP molecules. To study the effect of the polymer chains, we have performed calculations by combining the P3HT and PVP monomers, dimers and trimers. The following discussion falls into three sections. In Section 2, we introduce the computational methods. In Section 3, we present our calculation results. In Section 4, we draw some general conclusions.

2 | COMPUTATIONAL METHODS

In Figure 2, we show our modelling procedure, which includes the calculations for individual P3HT and PVP molecules, and the combination of their monomers, dimers and trimers. Gaussian 09[37] has been used with different functionals to compute the electronic structures of the molecules aforementioned. We have chosen the functionals at difference theoretical levels, including Hartree-Fock (HF), PBE,[38] BLYP,[39,40] B3LYP-ED2,[41] B3LYP-ED2 and B3LYP-ED3 for a comparison.[42] HF only takes into account the Coulomb and exchange interactions, PBE is the generalised gradient approximation (GGA) to the exchange-correlation functional and B3LYP combines the GGA functional BLYP[39,43] with the exact exchange using three empirical fitting parameters to balance the charge delocalization and localization. On top of B3LYP and BLYP, we can include the empirical dispersion (ED) forces at different levels through B3LYP-ED2 (and BLYP-ED2) and ED3. The basis set used was 6-31G—mostly commonly applied one in other simulations. In addition to the ground-state single-point calculations, the optimised molecular structure and the related orbitals are also of great interests because these are strongly related to the electron transport and optical properties. We have taken into account the basis set superposition error (BSSE) by using the counterpoise method implemented in Gaussian 09.[44] In the counterpoise method, the BSSE is computed as the difference between the total energies with mixed basis set and monomers. Another method is the chemical Hamiltonian approach, in which the basis set mixing is prevented through projectors.[45] The two approaches for BSSE would give similar results.[46] CrystalMaker and Avogadro[47,48] were used complimentarily to manipulate and visualise molecular structures. The atomic unit (a.u.) was used throughout all the calculations. The P3HT and PVP monomer, dimer and trimer were computed as an approximation to the polymers. In Figure 1C, we illustrate the integrated molecular structure of P3HT and PVP monomers. Here, we also define that the *z*-direction is perpendicular to the molecular plane, whereas *x*- and *y*-directions are in the molecular plane, as shown in Figure 1C. Regarding the colour coding for the atoms, hydrogen is in white, carbon is in grey, oxygen is in red and sulphur is in yellow. For molecular wave functions, such as the highest occupied molecular orbital (HOMO) and lowest unoccupied molecular orbital (LUMO), the positive sign is depicted as red and negative as blue. We have computed the inter-molecular interaction energy in terms of adsorption energies, defined as the

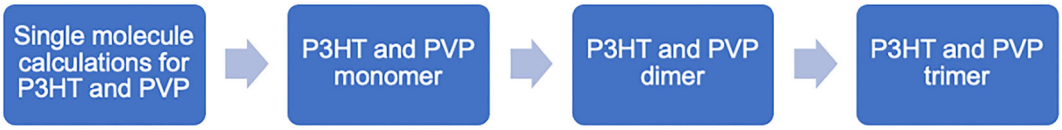

FIGURE 2 A flowchart for our molecular simulation process. PVP, povidone; P3HT, poly(3-hexylthiophene).

difference between the total energies of the combined molecule (E_{Combined}) and those for the individual molecules ($E_{\text{P3HT}} + E_{\text{PVP}}$).

$$E_{\text{interaction}} = E_{\text{Combined}} - (E_{\text{P3HT}} + E_{\text{PVP}}) \quad (1)$$

Then we varied the distance between P3HT and PVP along the *z*- (vertical distance) and x-directions (the sliding effect) and performed geometry optimization to work out the adsorption energies and optimal distances. In addition, we have compared BSSE with the adsorption energy computed. The optimal distances have been determined by using BLYP + ED2 and B3LYP + ED2, which have been compared to assess the performance of the functionals.

3 | RESULTS AND DISCUSSIONS

We compared the calculation results for the monomer calculations based on different functionals, including HF, PBE, B3LYP, B3LYP-ED2 and B3LYP-ED3 (not shown). Our calculations suggested that HF has a poor estimation, PBE was a better choice but may not be suitable for the polymers and B3LYP is the most appropriate one among all three, in the sense of the ground-state total energies. In addition, we can see the structural optimization either partially or for all the atoms will also lower the total energies. Notice that we did not perform the calculations for B3LYP-ED2 and B3LYP-ED3 without optimization or with partial optimization as these calculations are only for comparison to choose the appropriate methods.

The differences between with and without the Grimme's corrections for dispersion forces are calculated for the combined monomer when changing the distance on different directions. Figure 3 shows for the combined monomers, without optimization and with partially optimization, how the convergence energy changed with intermolecular distance, with pure B3LYP functionals, as well as ED2 and ED3 corrections. When the inter-molecule distance is small, especially at around the optimum distance, the convergence energy calculated with the 'fr' method (the coordinates of a part of molecule are frozen to ease the optimization) gave lower values, which implied more stable structures, as expected. As a result, only the partial optimization would be applied for further discussion.

From Figure 3, the trends for the calculations with the Grimme's correction for the total energies were similar to those without the correction, and the overall convergence energy tended to be lower, notwithstanding the distance. Interestingly, Figure 3 showed that the ED2 approximation can result in a lower energy than ED3, which could be due to the overall repulsion energies originating from the three-body interaction terms (ED3). Here, we neglected the three-body interaction and performed all the remaining calculations by using B3LYP/BLYP + ED2.

The adsorption energies for different conditions were calculated using the Equation (1) in Section 2. They all followed the trend of a dramatic decrease in adsorption energy first at small intermolecular distance, then a steady increase with larger distance. The results from this research were collected in Figures 4, 5 and 6, which are corresponding to the combined monomer, dimer and trimer, respectively. Besides, the optimization distances on the vertical direction and their optimization energies are listed in Table 1. As discussed in the previous subsection, all the results were generated using B3LYP/BLYP-ED2.

The initial distance of 2.8 Å was a good choice for the combined monomer (similar to the inter-plane distance

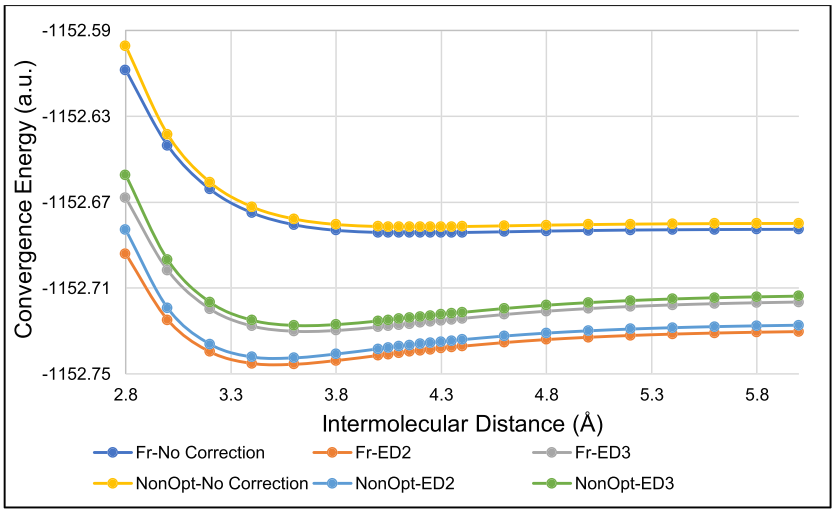

FIGURE 3 Convergence energy of the combined poly(3-hexylthiophene) (P3HT) and povidone (PVP) monomers, changing with distance using different Grimme's corrections without optimization (NonOpt) and when freezing a part of the molecule (Fr).

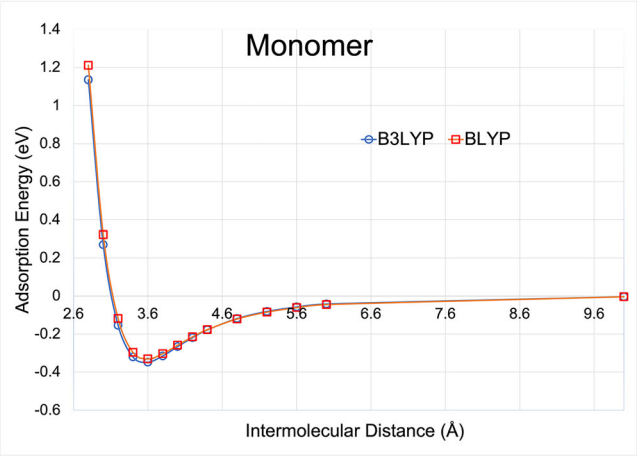

FIGURE 4 Adsorption energies vary with the intermolecular distance in a combined poly(3-hexylthiophene) (P3HT) and povidone (PVP) monomers, computed by using B3LYP + ED2 (blue circles) and BLYP + ED2 (red squares).

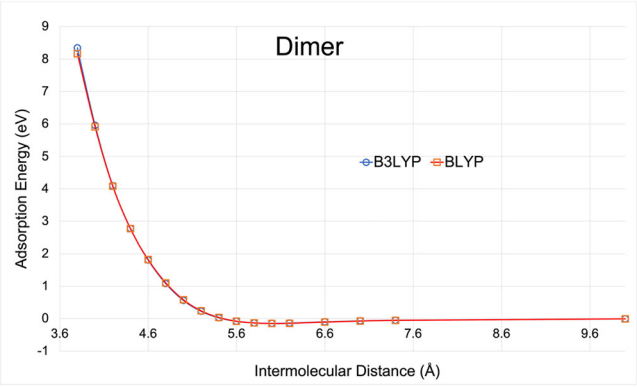

FIGURE 5 Adsorption energies as a function of the intermolecular distance in a combined poly(3-hexylthiophene) (P3HT) and povidone (PVP) dimers.

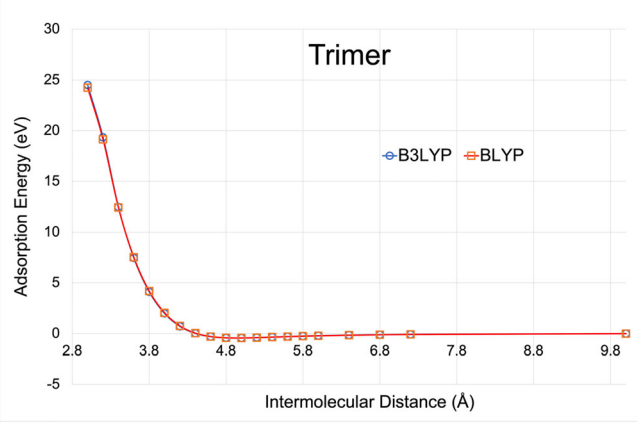

FIGURE 6 Adsorption energies as a function of the intermolecular distance in a combined poly(3-hexylthiophene) (P3HT) and povidone (PVP) trimers.

in graphite). As shown in Figure 4, with the increments of 0.2 and 0.4 Å, the lowest adsorption energy −0.35 (−0.33) eV occurred at ∼3.6 Å for monomer by B3LYP + ED2 (BLYP + ED2). Here, we can see that the value computed using B3LYP is lower by 0.02 eV. However, unlike the combined monomer, it turned out that the optimal inter-molecular distance for dimer was approximately 6.0 Å computed by both B3LYP + ED2 and BLYP + ED2. The adsorption energies are similar (−0.15 eV for B3LYP and −0.16 for BLYP). As we can see from Figure 5, the potential well around the optimal inter-molecular distance in the dimer calculations is much shallower than that for monomer. However, one cannot imply that with longer chains, the optimization dislocation can happen at further distance with more stable structure, which will be studied in the future work.

Taking the experience from the combined dimer, the distance domain was expanded to 3 to 10 Å for the trimer calculations (Figure 6). The optimal inter-molecular distance was then discovered at 5 Å, which is more acceptable than that of dimer, with the lower energy as −0.45 eV and the potential well is quite shallow as well. The higher optimum energy comparing with the monomer may be because of the curved backbone of the trimer. One extra difference from the combined monomer was the slope of energy declining before the optimization distance, which may be due to the hydrogen bonds between the hydrogen atoms of the P3HT and PVP molecules. With longer chains, the number of hydrogens is raising, which may lead to more hydrogen bonds built in this combined structure. As a result, the stabilisation speed became faster. However, with more carbon presenting, stronger repulsing force may occur in this structure. With the combination of both forces, the lowest energy would be increased, thus resulting in the less stable structure. The shallow potential well around the optimal inter-molecular distance for dimer and trimer implies that the interface is subject sensitively to all kinds of excitations such as vibrations. This will make the material interface unstable against the external stimulus. We can also see that the potential curve of this type would be useful for the analysis of material interface stability for OTFT.

In Figure 7, we show the ratio between the BSSE and the absolute value of adsorption energies as a function of inter-molecular distance. As expected, this ratio will take large value when the adsorption energies go through zero. At the optimal distances, BSSE contributed to ∼20%–30% error. The ratios for monomer, dimer and trimer are ∼30%, ∼20% and ∼25%, respectively, where B3LYP + ED2 and BLYP + ED2 provide very similar results with the results based on BLYP + ED2 slightly higher. These ratios suggest that the BSSE should be

Molecule chain length	Distance (Å)	Optimal adsorption energy (eV)	
		B3LYP	BLYP
Monomer	3.6	−0.35	−0.33
Dimer	6.0	−0.15	−0.16
Trimer	5.0	−0.45	−0.45

TABLE 1 The optimal intermolecular distance as a function of the polymer chain lengths.

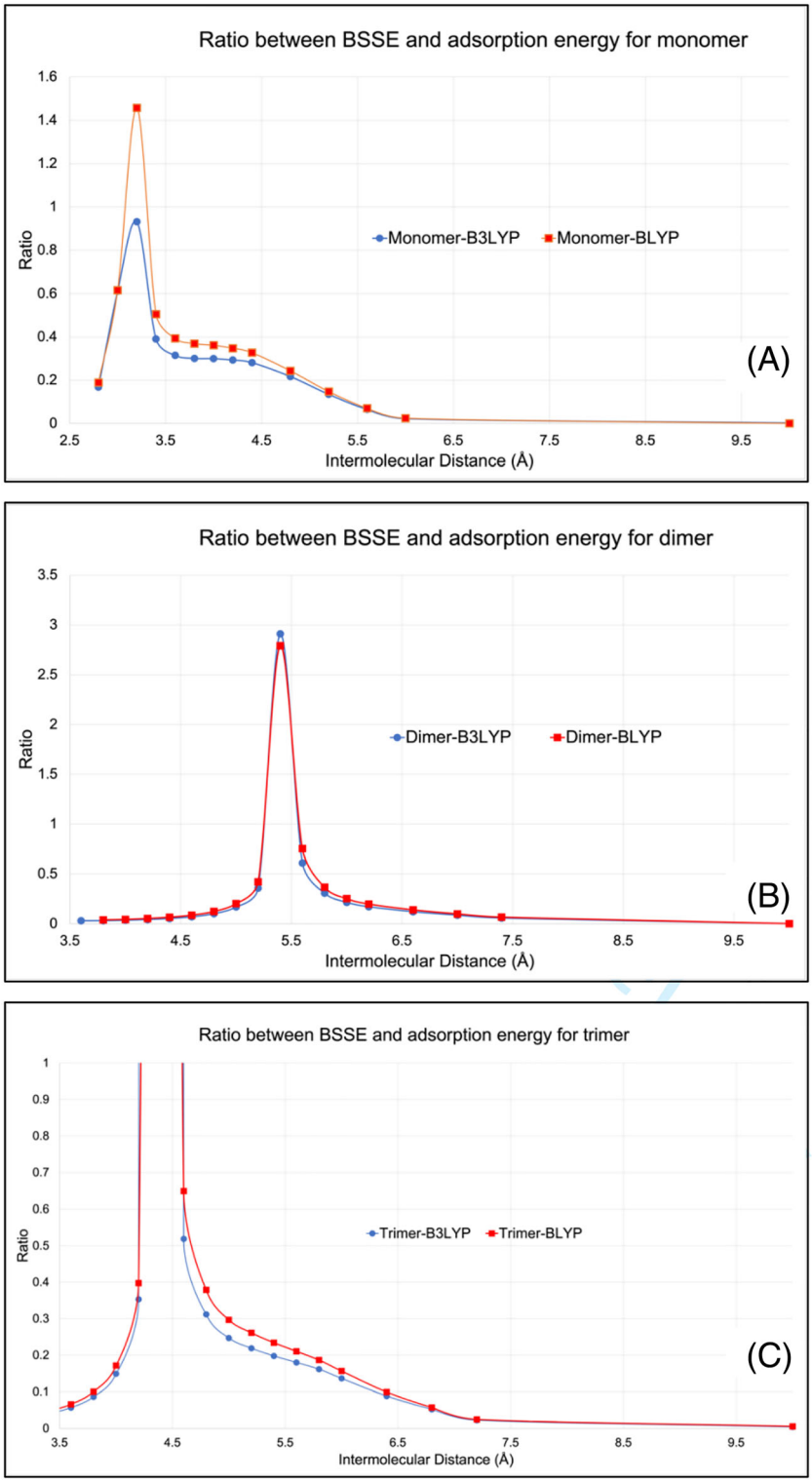

FIGURE 7 The ratios of basis set superposition error (BSSE) to the absolute values of adsorption energies as a function of inter-molecular distances for monomer (A), dimer (B) and trimer (C). For trimer, we only plotted up to the ratio of 1 to clearly illustrate the other ratios.

always taken into account when computing the adsorption energies for the combination of molecular fragments. As expected, the BSSE contribution will become smaller when the inter-molecular distance is large.

So far, all the distances have been defined along the vertical (z) axis. To be more rigorous, similar calculations were performed on the x- and y-directions. The adsorption energy is plotted in Figure 8, in which the adsorption

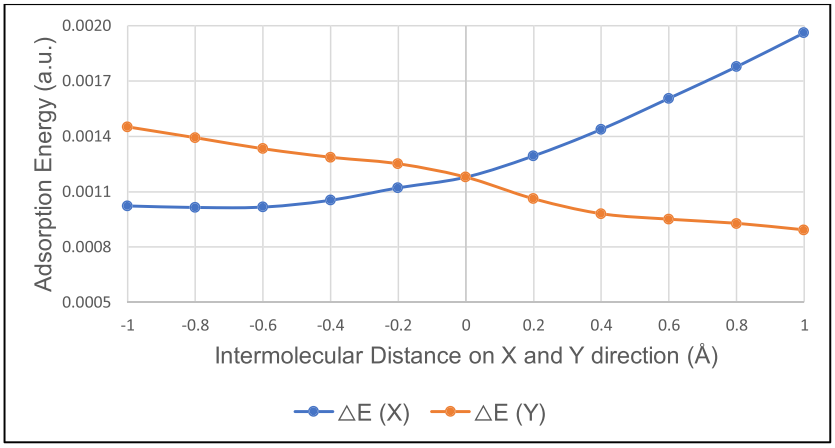

FIGURE 8 Adsorption energies varying as a function of the intermolecular distance along the X and Y directions in a combined poly(3-hexylthiophene) (P3HT) and povidone (PVP) monomers.

TABLE 2 Molecular orbitals for P3HT and PVP individual molecules.

Orbitals	P3HT	PVP
LUMO + 1	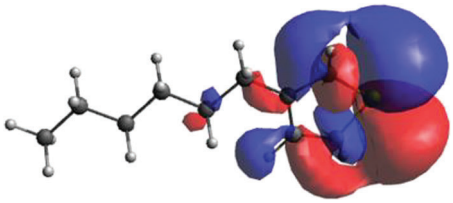	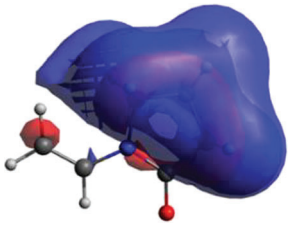
LUMO	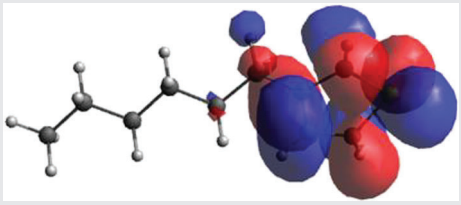	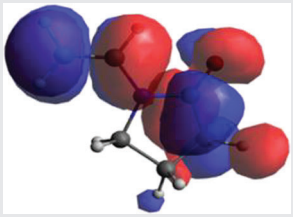
HOMO	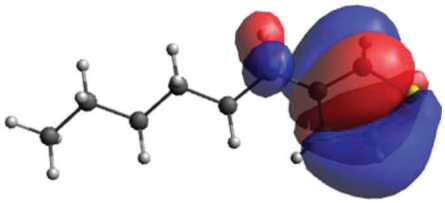	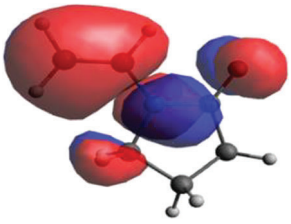
HOMO − 1	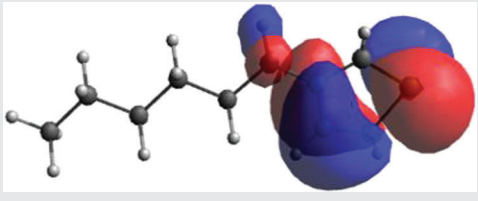	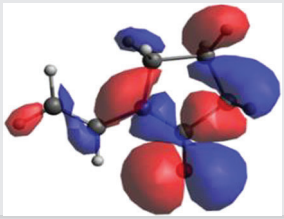

Abbreviations: HOMO, highest occupied molecular orbital; LUMO, lowest unoccupied molecular orbital; P3HT, poly(3-hexylthiophene); PVP, povidone.

TABLE 3 Molecular orbitals for combined molecules.

Orbitals	Monomer	Dimer	Trimer
LUMO + 1	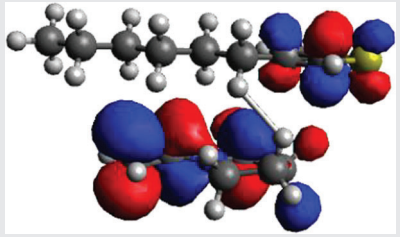	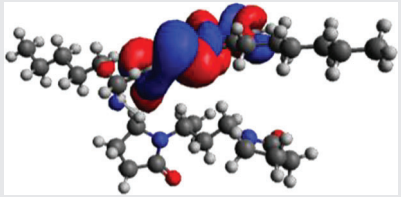	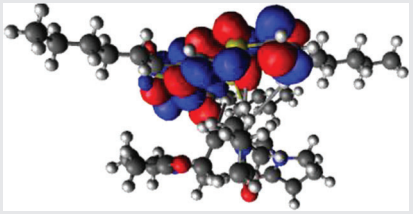
LUMO	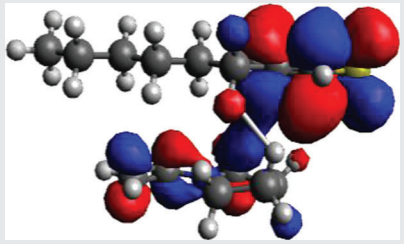	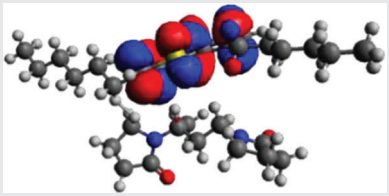	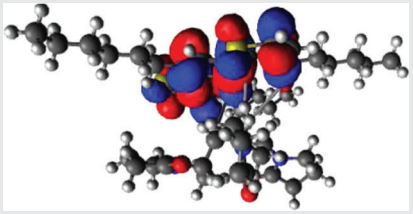
HOMO	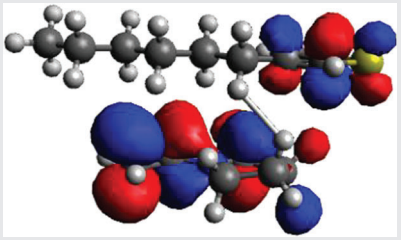	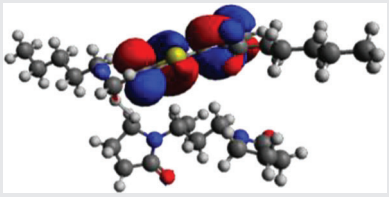	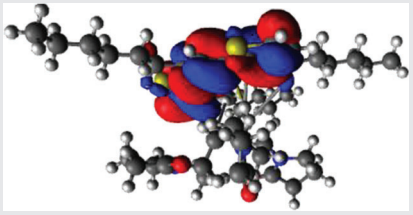
HOMO − 1	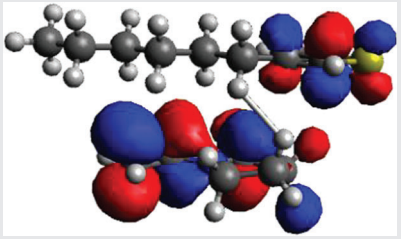	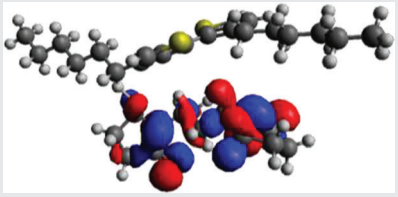	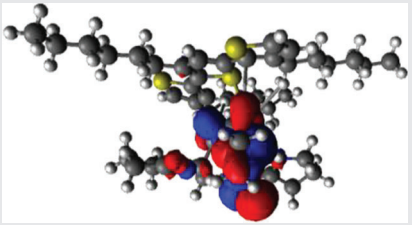

Abbreviations: HOMO, highest occupied molecular orbital; LUMO, lowest unoccupied molecular orbital.

energies for the P3HT and PVP monomers vary as a function of the intermolecular distance in the *x*- and *y*-directions. When one molecule is sliding on the *x*-*y* plane, the energy will have a fixed trend, either keep increasing (decreasing) with a very small energy (one order lower than the adsorption energy computed for the monomers) along *x* (*y*) direction. The adsorption energy was not same at opposite dislocations because of the asymmetry configuration of the two molecules along either *x*- or *y*-direction. Besides, in the practical application, the layers will extend along the plane, so the sliding effect is not as vital as the vertical distance. Therefore, no further simulation was made to the combined dimer and trimer.

We have also shown the molecular orbitals for individual P3HT and PVP molecules between HOMO − 1 and LUMO + 1 in Table 2. The electronic charge density is mainly on the five-member conjugated rings for both P3HT and PVP. For the combined molecules with large inter-molecular distance (Table 3), we can see the similar patterns for the distribution of the charge. From the optimised molecular structures, we can also see that the π-conjugated rings have been distorted due to the interactions between P3HT and PVP, which will have an important influence on the electrical properties such as the carrier mobility. The results for the optimal distance might be compared with the related experiments indirectly or directly through a few routes. One is to observe directly the crystal structure by using x-ray diffraction or nuclear magnetic resonance. In addition, scanning tunning microscopy and tunnelling electron microscopy might also be useful to observe the interface properties such as the molecular distance. The other route is to investigate the vibrational mode and the optical properties of the integrated molecular structures, which can be performed by using Fourier transformed infrared and ultraviolet-visible spectroscopies, respectively.

4 | CONCLUSIONS

In summary we have studied the interactions of the molecules P3HT and PVP, in two main layers—the semiconductor layer and the insulator layer, respectively, in the OTFT from a microscopic perspective. We have compared different theoretical methods (mainly B3LYP and BLYP) and found the optimised vertical intermolecular distance between two materials. We have also taken into account the BSSE and dispersion forces. Some limitations do exist during the calculation and analysis, but the overall results, especially the potential curve, can be useful for designing OTFT.

First, this simulation used different approximation methods, so difference functionals were compared, including the HF method, the PBE functionals and the hybrid-exchange B3LYP functionals. To make up the shortcomings of the B3LYP functionals, EDs, considered by two versions of Grimme's corrections (ED2 and ED3) were included. The energies from ED2 were lower than those from ED3, which could suggest the three-body repulsion energy. Additionally, the interesting trend of molecular orbitals was found, which provided the explanation for some strange points appeared in the optimization. The optimised intermolecular distances for the combined monomer, dimer and trimer are 3.6 (3.6), 6.0 (6.0) and 5.0 (5.0) Å, respectively, with the lowest adsorption energies of −0.35 (−0.33), −0.15 (−0.16) and −0.45 (−0.45) eV for B3LYP (BLYP) + ED2 + BSSE, respectively. The curved PVP long chain found from the optimised molecular structure contributed to the abnormal values for the combined dimer. Moreover, the last findings on the sliding effect do not seem to be as important as that on vertical dislocation (along the *z* direction), although it does follow certain patterns.

In the future, it is suggested to extend the chain to polymer to study it from a macro perspective and support actual applications. Besides, P3HT and PVP were found not to be the only outstanding organic semiconductor and insulator material. One can make this study as the reference for similar research using other materials. Except for these two layers interested, other layers in the OTFTs such as source and drains are also vital for the device performance. Therefore, the interactions among these and other layers can also be studied. Besides, one need to keep considering the effect of the electric dipole in the semiconductor while using the results from this study, because this is another property strongly dependent on the intermolecular distance.

Further limitations exist from the theories themselves. The lowest energy was always taken as the best approximation. However, there might be a chance of overestimation. Under that condition, the best estimation might not be from the lowest energy. This might be the reason why in this project ED2 correction is always better than ED3. The conclusion may reverse if the ED2 has overestimated. Apart from that, the semiconductor material can make contact with the insulator material with not only face-on orientation but also edge-on orientation, which can be studied in detail in the future. Other additional simulation can also be made related to this research. One typical example could be the dynamical simulation for molecular motions, which is important for the real-world applications of the wearables. As stated, all the results from this paper were based on the quantum mechanical theories, which included varieties of approximations. Hence, it is critical to compare the simulation results with the relevant experimental works.

ACKNOWLEDGEMENTS

We thank the UCL research computing team for their support. WW would like to acknowledge the funding support from EU Marketplace project 545083.

ORCID

Wei Wu https://orcid.org/0000-0003-2843-5113

REFERENCES

[1] M. Mizukami, N. Hirohata, T. Iseki, K. Ohtawara, T. Tada, S. Yagyu, T. Abe, T. Suzuki, Y. Fujisaki, Y. Inoue, S. Tokito, T. Kurita, *IEEE Electron. Dev. Lett.* **2006**, *27*(4), 249.

[2] E. Cantatore, T. C. T. Geuns, G. H. Gelinck, E. V. Veenendaal, A. F. A. Gruijthuijsen, L. Schrijnemakers, S. Drews, D. M. De Leeuw, *IEEE J. Solid-State Circuits.* **2007**, *42*(4), 84.

[3] M. Takamiya, T. Sekitani, Y. Kato, H. Kawaguchi, *IEEE J. Solid-State Circuits.* **2007**, *42*(1), 93.

[4] D. Tobjork, R. Osterbacka, *Adv. Mater.* **2011**, *23*(17), 1935.

[5] D. R. Seshadri, J. R. Rowbottom, C. Drummond, J. E. Voos, J. Craker, *2016 8th Cairo International Biomedical Engineering Conference (CIBEC)*, IEEE, Cairo, Egypt **2016**, pp. 52-55. https://doi.org/10.1109/CIBEC.2016.7836118

[6] F. Mokhtar, Z. Cheng, R. Raad, J. Xi, J. Foroughi, *J. Mater. Chem. A* **2020**, *8*, 9496.

[7] Anon, Sensor technology and applications. ECS, **2016**, https://www.electrochem.org/world-of-sensors/ (accessed: August 2021).

[8] T. Sekitani, U. Zschieschang, H. Klauk, T. Someya, *Nat. Mater.* **2010**, *9*(12), 1015.

[9] T. Sekitani, S. Iba, Y. Kato, Y. Noguchi, T. Someya, T. Sakurai, *Appl. Phys. Lett.* **2005**, *87*(17), 173502.

[10] Y. Zhou, S. T. Han, V. A. L. Roy, *Nanocrystalline Materials*, Elsevier **2014**, 195.

[11] S. R. Puniredd, W. Pisula, K. Müllen, *Woodhead Publ. Ser. Electron. Opt. Mater* **2013**, *39*, 83.

[12] K. P. Goetz, O. D. Jurchescu, *Handbook of Organic Materials for Electronic and Photonic Devices*, Woodhead Publishing **2019**, 453.

[13] A. J. Bandodkar, I. Jeerapan, J. Wang, *Acs Sens.* **2016**, *1*(5), 464.

[14] X. Z. Wang, S. H. Masood, *Mater. Des.* **2011**, *32*(3), 1118.

[15] Anon, Poly(3-hexylthiophene-2,5-diyl). Poly(3-hexylthiophene-2,5-diyl) - P3HT. https://www.sigmaaldrich.com/CA/en/substance/poly3hexylthiophene25diyl12345156074985?context=product (accessed: January 2021).

[16] Anon, Polyvinylpyrrolidone average mol WT 40,000: SIGMA-ALDRICH, average mol wt 40,000 | 9003-39-8. https://www.sigmaaldrich.com/CA/en/product/sial/pvp40 (accessed: March 2021).

[17] T. G. Bäcklunda, R. Österbacka, H. Stubb, *J. Appl. Phys.* **2005**, *98*, 074504.

[18] C. D. Dimitrakopoulos, D. J. Mascaro, *IBM J. Res. Dev.* **2001**, *45*, 11.

[19] C. G. Kuo, J. H. Chen, Y. C. Chao, P. L. Chen, *Sensors* **2018**, *18*(1), 37.

[20] S. Hou, J. Yu, X. Zhuang, D. Li, Y. Liu, Z. Gao, T. Sun, F. Wang, X. Yu, *ACS Appl. Mater. Interfaces* **2019**, *11*(47), 44521.

[21] B. Aïssa, A. Ali, A. Bentouaf, W. Khan, M. I. Hossain, J. Kroeger, N. M. Muhammad, *Nanotechnology* **2019**, *31*(7), 075201.

[22] X. Zhang, B. Wang, L. Huang, W. Huang, Z. Wang, W. Zhu, Y. Chen, Y. Mao, A. Facchetti, T. J. Marks, *Sci. Adv.* **2020**, *6*(13), eaaz1042.

[23] J. I. Lee, M. Kim, J. H. Park, B. Kang, C. Y. Lee, Y. D. Park, *ACS Appl. Mater. Interfaces* **2021**, *13*, 24005.

[24] M. Mas-Torrent, D. Den Boer, M. Durkut, P. Hadley, A. P. Schenning, *Nanotechnology* **2004**, *15*(4), S265.

[25] Z. Bao, A. Dodabalapur, A. J. Lovinger, *Appl. Phys. Lett.* **1996**, *69*(26), 4108.

[26] S. Oh, R. Hayakawa, C. Pan, K. Sugiyasu, Y. Wakayama, *J. Appl. Phys.* **2016**, *120*(5), 055501.

[27] F. Zare Bidoky, W. J. Hyun, D. Song, C. D. Frisbie, *Appl. Phys. Lett.* **2018**, *113*(5), 053301.

[28] S. Nam, J. Seo, H. Kim, Y. Kim, *Appl. Phys. Lett.* **2015**, *107*(15), 97_1.

[29] Y. J. Song, J. U. Lee, W. H. Jo, *Carbon* **2010**, *48*(2), 389.

[30] X. Guo, Y. Xu, S. Ogier, T. N. Ng, M. Caironi, A. Perinot, L. Li, J. Zhao, W. Tang, R. A. Sporea, A. Nejim, *IEEE Trans. Electron. Dev.* **2017**, *64*(5), 1906.

[31] W. Boukhili, C. Tozlu, R. Bourguiga, S. Wageh, *Chinese J. Phys.* **2018**, *56*(5), 1964.

[32] C. Koutsiaki, T. Kaimakamis, A. Zachariadis, S. Logothetidis, *Mater. Today: Proc.* **2019**, *19*, 58.

[33] P. Xie, T. Liu, P. He, G. Dai, J. Jiang, J. Sun, J. Yang, *Sci. China Mater.* **2020**, *63*(12), 2551.

[34] M. H. Yoon, H. Yan, A. Facchetti, T. J. Marks, *J. Am. Chem. Soc.* **2005**, *127*(29), 10388.

[35] J. Li, W. Tang, Q. Wang, W. Sun, Q. Zhang, X. Guo, X. Wang, F. Yan, *Mater. Sci. Eng. R Rep.* **2018**, *127*, 1.

[36] J. Choi, J. Yoon, M. J. Kim, K. Pak, C. Lee, H. Lee, K. Jeong, K. Ihm, S. Yoo, B. J. Cho, H. Lee, *ACS Appl. Mater. Interfaces* **2019**, *11*(32), 29113.

[37] M. J. Frisch, G. W. Trucks, H. B. Schlegel, G. E. Scuseria, M. A. Robb, J. R. Cheeseman, G. Scalmani, V. Barone, B. Mennucci, G. A. Petersson, H. Nakatsuji, M. Caricato, X. Li, H. P. Hratchian, A. F. Izmaylov, J. Bloino, G. Zheng, J. L. Sonnenberg, M. Hada, M. Ehara, K. Toyota, R. Fukuda, J. Hasegawa, M. Ishida, T. Nakajima, Y. Honda, O. Kitao, H. Nakai, T. Vreven, J. A. Montgomery, J. E. Peralta Jr., F. Ogliaro, M. Bearpark, J. J. Heyd, E. Brothers, K. N. Kudin, V. N. Staroverov, T. Keith, R. Kobayashi, J. Normand, K. Raghavachari, A. Rendell, J. C. Burant, S. S. Iyengar, J. Tomasi, M. Cossi, N. Rega, J. M. Millam, M. Klene, J. E. Knox, J. B. Cross, V. Bakken, C. Adamo, J. Jaramillo, R. Gomperts, R. E. Stratmann, O. Yazyev, A. J. Austin, R. Cammi, C. Pomelli, J. W. Ochterski, R. L. Martin, K. Morokuma, V. G. Zakrzewski, G. A. Voth, P. Salvador, J. J. Dannenberg, S. Dapprich, A. D. Daniels, O. Farkas, J. B. Foresman, J. V. Ortiz, J. Cioslowski, D. J. Fox, *Gaussian 09*, Revision D.01, Gaussian Inc., Wallingford (CT) **2013**.

[38] J. P. Perdew, K. Burke, M. Ernzerhof, *Phys. Rev. Lett.* **1996**, *77*, 3865.

[39] A. D. Becke, *Phys. Rev. A* **1988**, *38*, 3098.

[40] B. Miehlich, A. Savin, H. Stoll, H. Preuss, *Chem. Phys. Lett.* **1989**, *157*, 200.

[41] A. D. Becke, *J. Chem. Phys.* **1993**, *98*, 5648.

[42] S. Grimme, *J. Comput. Chem.* **2006**, *27*, 1787.

[43] C. Lee, W. Yang, R. G. Parr, *Phys. Rev. B* **1988**, *37*, 785.
[44] S. Simon, M. Duran, J. J. Dannenberg, *J. Chem. Phys.* **1996**, *105*, 11024.
[45] I. Mayer, P. Valiron, *J. Chem. Phys.* **1998**, *109*, 3360.
[46] B. Paizs, S. Suhai, *J. Comput. Chem.* **1998**, *19*, 575.
[47] D. C. Palmer, *CrystalMaker*, CrystalMaker Software Ltd, Begbroke, Oxfordshire, England **2014**.
[48] M. D. Hanwell, D. E. Curtis, D. C. Lonie, T. Vandermeersch, E. Zurek, G. R. Hutchison, *J. Cheminformatics* **2012**, *4*, 17.

How to cite this article: X. Du, W. Wu, K.-L. Choy, *J Phys Org Chem* **2023**, e4494. https://doi.org/10.1002/poc.4494